



ORIGINAL ARTICLE

Synthesis of new 1,2,3-triazole linked benzimidazolidinone: Single crystal X-ray structure, biological activities evaluation and molecular docking studies



Hanan Al-Ghulikah^{a,*}, Ameni Ghabi^b, Amel haouas^c, Hasan Mtiraoui^b,
Erwann Jeanneau^d, Moncef Msaddek^b

^a Department of Chemistry, College of Science, Princess Nourah bint Abdulrahman University, P.O. Box 84428, Riyadh 11671, Saudi Arabia

^b Laboratory of Heterocyclic Chemistry Natural Products and Reactivity/CHPNR, Department of Chemistry, Faculty of Science of Monastir, University of Monastir, 5000 Monastir, Tunisia

^c Department of Chemistry, Faculty of Science, Northern Border University, Arar, Saudi Arabia

^d Université Lyon1, Institut de Chimie de Lyon, Centre de Diffractométrie Henri Longchambon, 69622 Villeurbanne, France

Received 7 August 2022; accepted 7 January 2023

Available online 11 January 2023

KEYWORDS

1,2,3-triazole-benzimidazolidinone;
CuAAC;
Antimicrobial;
Anti-inflammatory;
Docking

Abstract A novel series of 1,2,3-triazole-benzimidazolidinone hybrid derivatives were designed and synthesized *via* click reaction, between various aryl azide and a terminal alkyne bearing a benzimidazolidinone moiety. All newly synthesized compounds, were efficiently characterized using ¹H NMR, ¹³C NMR and HRMS. Furthermore, the structure of one precursor **5b** was supported by single crystal X-ray diffraction. All synthesized derivatives have been evaluated for their antimicrobial and anti-inflammatory activities. Biological activity tests exhibited that the target structures demonstrate that compounds **5a**, **5b** and **5f** have a high antibacterial activity especially derivative **5b**. Besides, the *in vitro* antifungal results revealed that the strongest inhibition recorded to compound **5b** in comparison to other products against *A. brasiliensis*, *A. fumigatus* and *C. albicans*. Biological activity evaluation indicated that the synthesized compounds possess moderate anti-inflammatory effects. The most effective compound in terms of efficacy and potency was **5a**. Molecular docking simulation was used to investigate the most active compounds' probable binding

* Corresponding author.

E-mail address: haalghulikah@pnu.edu.sa (H. Al-Ghulikah).

Peer review under responsibility of King Saud University.



Production and hosting by Elsevier

mechanisms in order to provide a plausible explanation for their biological activity.

© 2023 The Authors. Published by Elsevier B.V. on behalf of King Saud University. This is an open access article under the CC BY-NC-ND license (<http://creativecommons.org/licenses/by-nc-nd/4.0/>).

1. Introduction

Benzimidazolone present a crucial heterocyclic building blocks that attracted special attention for their pronounced therapeutic applications. The majority of the studies show that benzimidazolone compounds exhibit a variety of pharmacological and biological properties including anti-HIV (Pribut et al., 2019), antinociceptive (Intagliata et al., 2020), cytotoxic (Banerji et al., 2015), antitrichinellosis (Mavrova et al., 2005), antiproliferative (El-Naggar et al., 2018), antituberculosis (Jagannath et al., 2021), antioxidant (Ibrahim et al., 2021) and antibacterial (Saber et al., 2021a).

As reported in literature, authors are interested currently in creating bioactive compounds with good pharmacokinetics features (Chamani et al., 2006), various drug administration (Atena et al., 2021), diversity of drug targeting (Nooshin et al., 2016), potent bioavailability (Narges et al., 2022), efficient pharmacological proper-

ties (Maryam et al., 2020), broad spectrum (Najmeh et al., 2021, Sattar et al., 2022), low toxicity, better curative impact (Reza et al., 2022), less adverse effects, have been showing more and more range of clinical applications for the treatment of different diseases (Hamid et al., 2022). In particular, many examples of drug molecules containing triazole ring are described including Triadimefon (Paredes-Zúñiga et al., 2019), Etizolam (Nielsen et al., 2020), Hexaconazole (Worthington, 1991), Triazolam (Miyata et al., 2014), Rizatriptan (Mujahid et al., 2021), Ribavirin (Khalili et al., 2020), Propiconazole (Valadas et al., 2019), Myclobutanil (Fonseca et al., 2020) Rufinamide (Panebianco et al., 2020), Fluconazole (Lu et al., 2021), Carboxyamidotriazole (Shi et al., 2022), Tazobactam (Tamma et al., 2021) Fig. 1.

Furthermore, the introducing of a triazole ring connected to different pharmacophore fragments can produce new bi/polyfunctional drug molecules. Indeed, 1,2,3-triazole hybrid have attracted the interest of medicinal chemists due to their broad spectrum of applications such

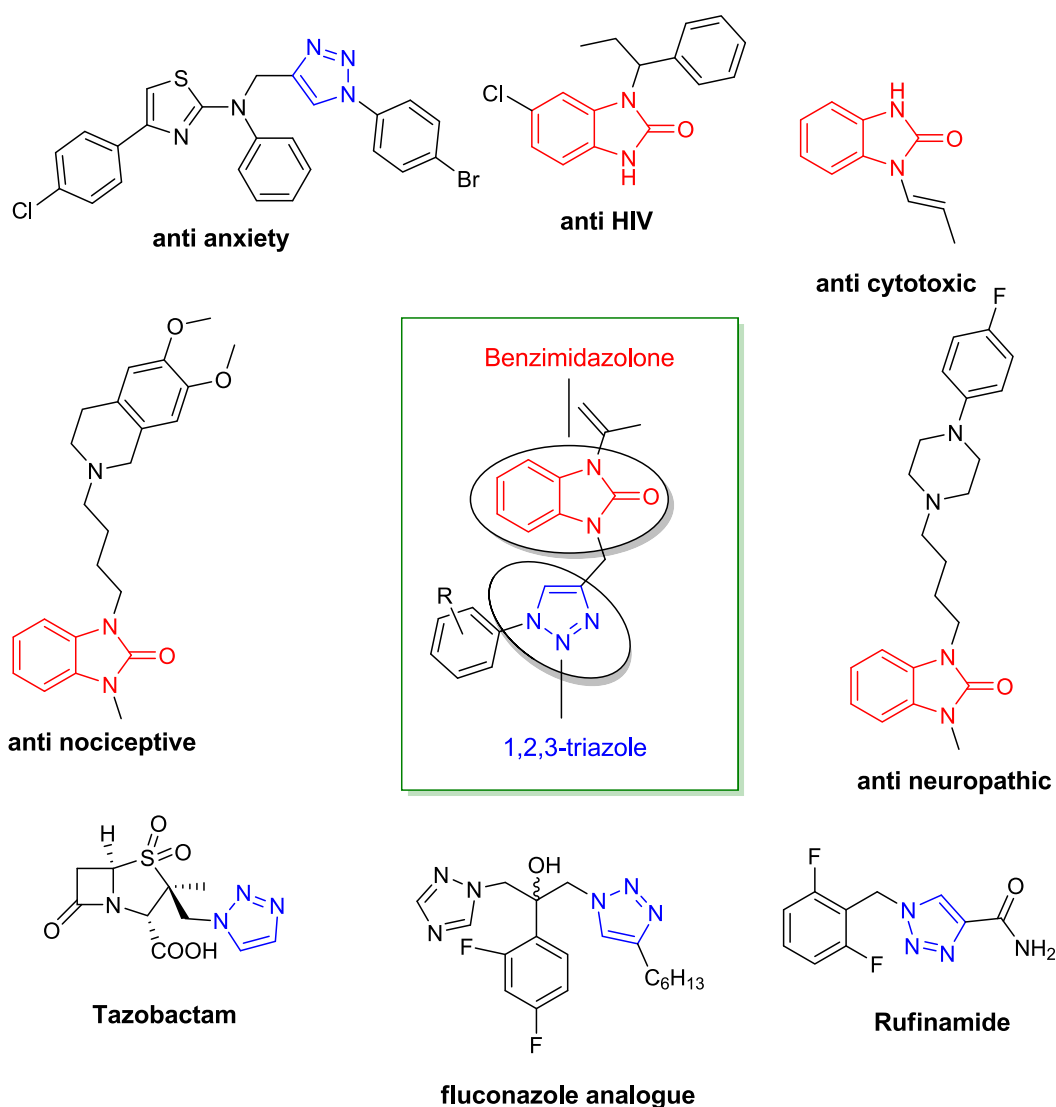


Fig. 1 Examples of active drugs containing triazole and benzimidazolone scaffold.

as anti-viral (Saroja et al., 2022), antitubercular (Harish, 2021), antimicrobial (Poonia et al., 2022), anti-HIV-1 (Feng et al., 2021), anti-alzheimer (Zahra et al., 2019), cholinesterase inhibitors (Rania et al., 2021) and antiproliferative agents (Arif et al., 2022). Therefore, the benzimidazolone linked triazole moiety has gained significant attention thanks to their biological properties (Saber et al., 2021b).

Furthermore, the synthesis of 1,2,3-triazole has been extensively researched for its pharmacological effects such as neuroprotective agents (Bozorov et al., 2019, Duarte et al., 2017), anti anxiety-anti-inflammatory (Ankali et al., 2021) antibacterial-antileishmanial (Çelik et al., 2021), antichagasic agents (Silva et al., 2021). Huisgen (Rolf et al., 1967) first outlined the reaction between azides and acetylenes as a way of synthesizing these heterocyclic molecules. Due to the high activation energy, these reactions necessitate a high temperature and a long reaction time, in addition to the creation of a mixture of 1,4- and 1,5-regioisomers (Ali et al., 2016). Cu catalyzed azide-alkyne cycloaddition process (CuAAC), also known as the Click reaction, was reported in 2002 to have 100 % regioselectivity (only the 1,4-disubstituted regioisomer is obtained) and excellent yield under mild, safe reaction conditions (Darroudi et al., 2021, Nemallapudi et al., 2021).

Due to the importance of these heterocyclic scaffolds and in connection with these findings, we are interested to prepare a new series of 1,2,3-triazole linked benzimidazolone and evaluating *in vitro* their biological properties including antimicrobial and anti-inflammatory activities. Significant findings have been made and the structure-activity relationship of these synthesized derivatives was also discussed and further demonstrated by molecular docking simulation.

2. Results and discussion

2.1. Synthesis

The synthesis of hybrid molecules was carried out in four steps. Our synthetic route begins by the preparation of the dipolarophile **3** obtained by propargylation reaction between propargyl bromide and 1-(prop-1-en-2-yl)-1H-benzo[d]imidazol-2(3H)-one **2** which has been prepared from *o*-phenylenediamine (OPDA) and ethylacetoacetate as starting materials (Scheme 1). The propargylation of **2** offers the appropriate terminal alkyne **3** in 80 % yield. The ¹H NMR spectrum of *N*-propargylated compound **3**, revealed the disappearance of NH signal at δ_H 10.87 ppm and the appearance of two new characteristic signals at δ_H 4.69 ppm and δ_H 2.31 ppm, assigned to the *N*-CH₂ and the alkyne protons of the propargyl unit, respectively.

In parallel, aryl azides **4a-f** were subjected to our “step-by-step” synthetic procedure, starting from the preparation of diazonium salt by reacting of various aniline with NaNO₂ (sodium nitrite) following via nucleophilic aromatic substitu-

tion reaction using NaN₃ (sodium azide) *in situ*. We have continued our work to synthesis 1,2,3-triazole by the 1,3-dipolar cycloaddition (CuAAC) starting from 1-(prop-1-en-2-yl)-3-(prop-2-yn-1-yl)-1H-benzo[d]imidazol-2(3H)-one **3** as a dipolarophilic system and aromatic azide **4a-f** (Kamalraj et al., 2008) using a catalytic amount of Copper(I) iodide to generate a novel series of 1,2,3-triazole derivatives **5a-f** in good yield (Scheme 2).

The physical properties of these structures are shown in Table 1.

A proposed reaction mechanism for the preparation of 1,2,3-triazole ring can be introduced in Scheme 3.

The structures of 1,2,3-triazole prepared **5a-f** were fully described by analytical techniques (¹H NMR, ¹³C NMR, RX, HRMS). ¹H NMR spectrum of compound **5c**, showed a characteristic triazolyl proton as a singlet at δ_H 7.63 ppm due to inductive effect. Furthermore, a sharp singlet assigned to methylene protons was revealed at δ_H 5.31 ppm and two a doublet of doublet exhibited in the range δ_H 5.21–5.36 ppm attributed to methylene (CH₂ =) and a triplet at δ_H 2.23 ppm corresponding to CH₃.

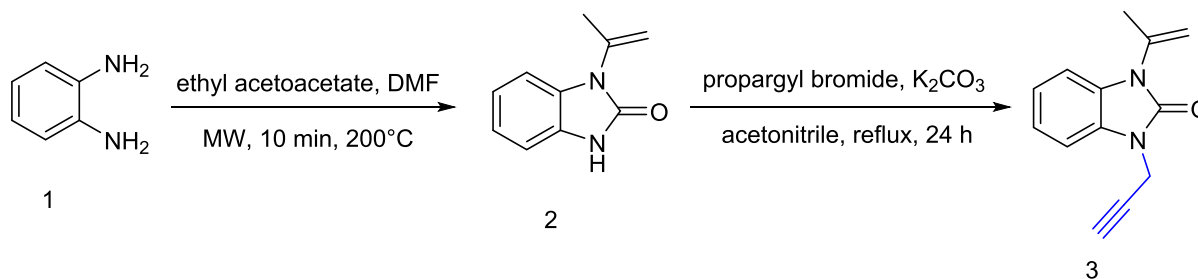
The analyse of ¹³C NMR spectrum of the cycloadducts **5a-f** displayed two characteristics signals corresponding to C-5 and the quaternary C-4 which appear at δ_C121.8 ppm and δ_C137.9 ppm respectively. All these observations confirm clearly the regioselectivity of the formation of 1,4-disubstituted 1,2,3-triazole scaffold. Furthermore, the structure and the regioselectivity were performed unambiguously by X-ray diffraction study applied on a single-crystal corresponding to compound **5b** as depicted in Fig. 2.

2.2. X-ray crystallographic study

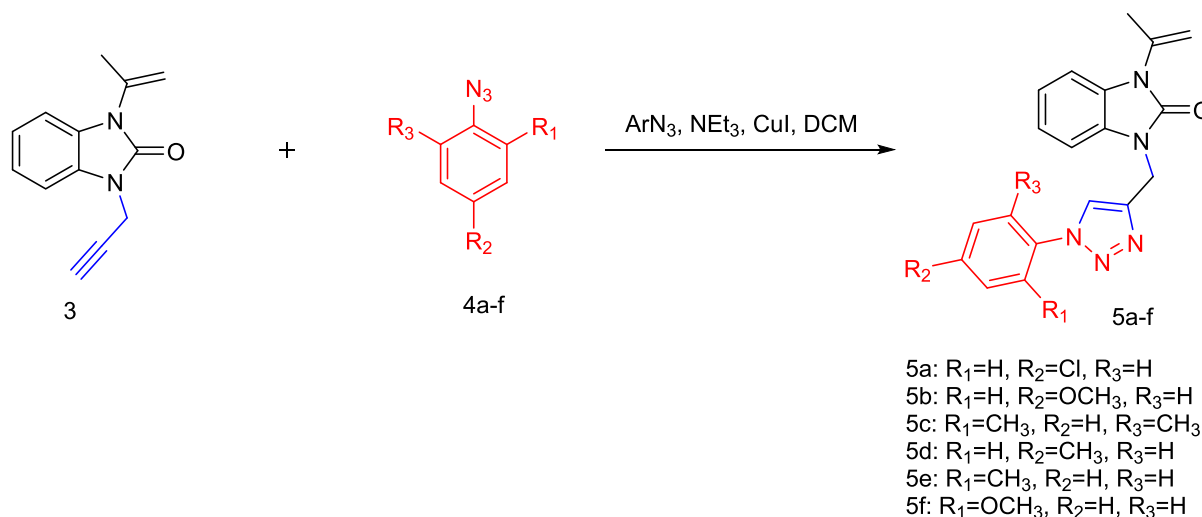
Single light yellow plate crystals of **5b** were used as supplied. A suitable crystal with dimensions 0.47 × 0.13 × 0.05 mm³ was selected and mounted on a nylon loop in perfluoroether oil on aXcalibur, Atlas, Gemini ultra diffractometer. The crystal was kept at a steady *T* = 150.00(10) K during data collection. The structure was solved with the ShelXT (Dolomanov et al., 2009) solution program using dual methods and by using Olex2 (Sheldrick et al., 2015a) as the graphical interface. The model was refined with ShelXL 2018/3 (Sheldrick et al., 2015b) using full matrix least squares minimization on *F*².

2.2.1. Crystal data

C₂₀H₁₉N₅O₂, *M_r* = 361.40, monoclinic, *I*2/*a* (No. 15), *a* = 16.4233(16) Å, *b* = 5.2305(5) Å, *c* = 40.413(6) Å, *b* = 93.973(11)°, *a* = *g* = 90°, *V* = 3463.3(7) Å³, *T* = 150.00



Scheme 1 General method for the synthesis of alkyne **3**.



Scheme 2 General method for the synthesis of triazole derivatives **5a-f**.

Table 1 Structures and yields of compounds **5a-f**.

Entry	Compd.	Substituent			Yields % ^a
		R ₁	R ₂	R ₃	
1	5a	H	Cl	H	74
2	5b	H	OCH ₃	H	68
3	5c	CH ₃	H	CH ₃	69
4	5d	H	CH ₃	H	70
5	5e	CH ₃	H	H	72
6	5f	OCH ₃	H	H	68

^a Isolated yield for the 1,2,3-triazole derivatives after purification by column chromatography.

(10) K, Z = 8, Z' = 1, $m(\text{Cu K}\alpha) = 0.758$, 15,059 reflections measured, 3076 unique ($R_{\text{int}} = 0.0494$) which were used in all calculations. The final wR_2 was 0.1231 (all data) and R_1 was 0.0451 ($I \geq 2 \sigma(I)$).

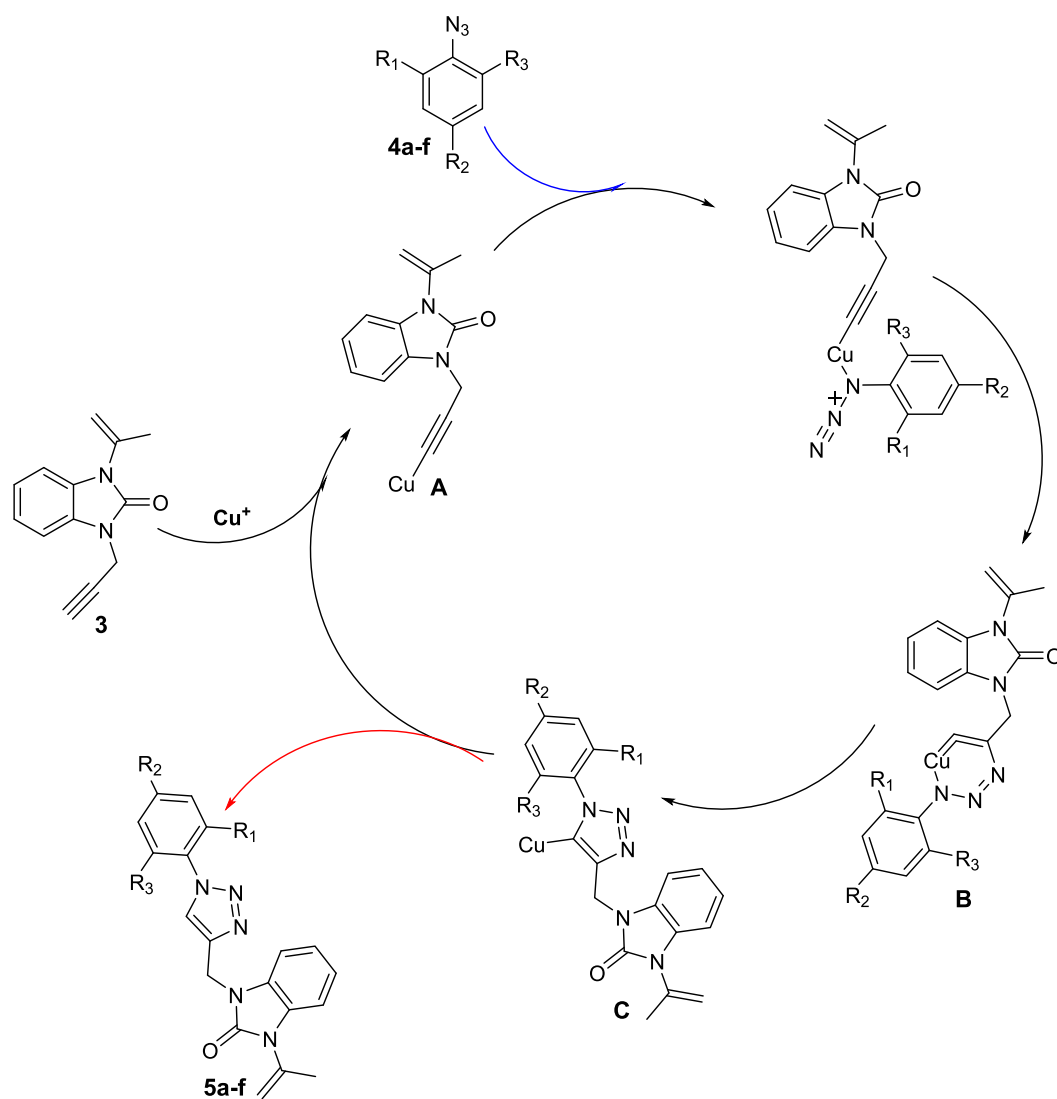
2.3. Biological activity and molecular modeling

2.3.1. Antibacterial activity

All the newly synthesized 1,2,3-triazole linked benzimidazolones derivatives **5a-f** were assessed in vitro against a variety of two Gram-positive bacteria (*S. aureus* and *B. subtilis*) and two Gram-negative bacteria (*S. typhi* and *E. coli*). By measuring the inhibition zone using well agar diffusion assay the activity of all the investigated compounds was compared to that of Ampicillin, which was utilized as a standard reference antibiotic (in mm). The inhibiting properties against these four strains are given in Table 2. It was found that the newly generated compounds **5a-f** have exerted globally moderate to good inhibitory activity against all of tested bacterial strains (IZ = 8 mm to 23 mm) compared to the reference antibiotic. In detail and starting with the inhibition effect towards gram positive bacteria; against *S. aureus*, based on zones of inhibition results and a part from the nature of the substituents in the *para*- and/or *ortho*-positions of the terminal phenyl, derivative **5f** by its *ortho*-methoxy group showed the highest activity (IZ = 19 mm) compared to the other compounds and Ampicillin (IZ = 17 mm) followed by compound **5b** with a methoxy group in the *para* position which displayed a zone of inhibition value equal to that of Ampicillin while **5c** (R = 2,6-diCH₃) and **5e** (R = 2CH₃) showed the lowest antibacterial effects (IZ = 9 mm, IZ = 8 mm respectively). This observation indicates the importance of methoxy groups in addition to triazole and benzimidazolone moieties for the *S. aureus* inhibition and the weak effect of methyl groups. Towards *B. subtilis*, derivatives **5b** (IZ = 19 mm) with its 4-OCH₃, **5a** (IZ = 18 mm) by its 4-Cl and **5f** (IZ = 17 mm) through its 2-OCH₃ groups exhibited the highest antibacterial potentials than the reference antibiotic (IZ = 14 mm) and other analogues. Furthermore, with regard to the Gram-negative bacteria: against *S. typhi* **5b** (IZ = 22 mm) was found to be the most active compound compared to its analogs followed by compounds **5a** (IZ = 21 mm) and **5f** (IZ = 20 mm). So, another time these three compounds showed greater inhibition potential than Ampicillin (IZ = 15 mm). In the same context towards *E. coli*, derivative **5b** besides to **5a** showed the highest antibacterial values followed by compound **5f** as Table 2 showed. Thus, based on the above findings, we can be inferred that the hybrid molecules combining the two fragments: 1-aryl-1H-1,2,3-triazole and benzimidazolone are considered to be a main skeleton for the design of new antibacterial compounds.

2.3.2. Molecular docking for antibacterial activity

A Molecular docking test is the finest approach to study the binding affinity of ligands against target protein to more explain the antibacterial activity (Horchani et al, 2020, Horchani et al, 2022a). To estimate the optimal conformational position within the active site of the targeted protein, all of the produced compounds **5a-f** were docked against: a crystal structure of a Gram-positive bacteria « Threonine synthase from *B. subtilis* ATCC 6633 » and a crystal structure of Gram-negative bacteria « MenB-1,4-dihydroxy-2-naphthoyl-CoA synthase from *E. coli* ATCC 25922 ». All the generated docked complexes were performed and analyzed on the basis of minimum energy values (kcal/mol) and hydrogen/hydrophobic interactions. All the created docked complexes were



Scheme 3 Proposed mechanism for synthesis of 1,2,3-triazole derivatives **5a-f**.

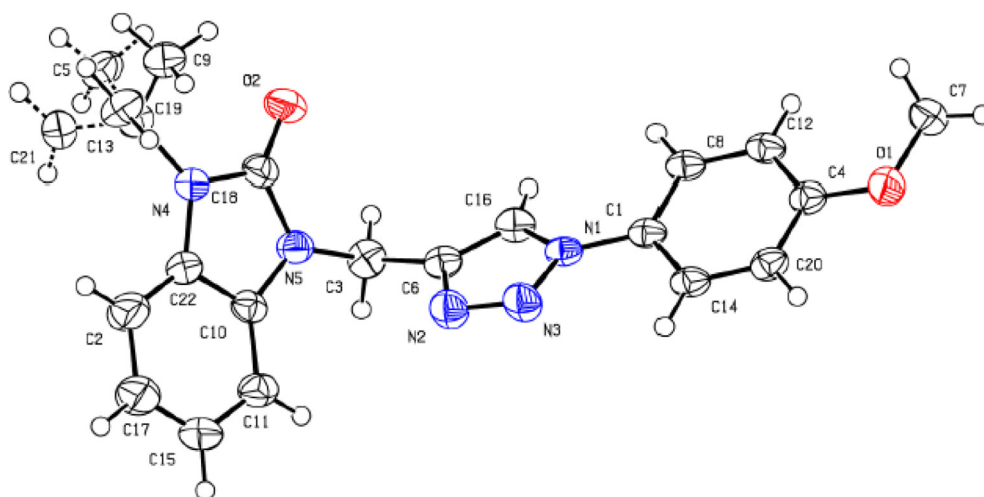


Fig. 2 Ortep diagram of the compound **5b**.

Table 2 Estimation of zone of inhibition of synthesized compounds against different bacterial strains.

Standard and Test compound	Zone of inhibition in mm			
	<i>S. aureus</i>	<i>B. subtilis</i>	<i>S. typhi</i>	<i>E. coli</i>
5a:4Cl	15	18	21	23
5b: 4OCH ₃	17	19	22	23
5c: 2,6-diCH ₃	9	11	14	13
5d:4CH ₃	10	10	12	13
5e: 2CH ₃	8	10	12	12
5f:2OCH ₃	19	17	20	22
Ampicillin	17	14	15	13

used to perform and analyze on the basis of minimum energy values (kcal/mol) and hydrogen/hydrophobic interactions.

From the docking results, as depicted in Table 3 and Fig. 3, against *B. subtilis*, compound **5b** having an interesting binding energy value is involved in two hydrogen bonds through its benzimidazolidinone and triazole fragment with THR83 and THR86 respectively. Additionally, a Pi-cation interaction is postulated with LYS59 by the *para*-methoxyphenyl group besides the appearance of some hydrophobic interactions with residues: PHE132 and ILE240. Thus, from the theoretical

Table 3 Docking binding energies (kcal/mol) of promising antibacterial agents.

Compound	Free binding energy of pdb: 6CGQ (kcal mol ⁻¹)	Free binding energy of pdb: 3 T88 (kcal mol ⁻¹)
5a	-7.8	-7.8
5b	-7.8	-7.9
5c	-7.4	-7.6
5d	-7.2	-7.7
5e	-7.6	-7.7
5f	-7.4	-7.8

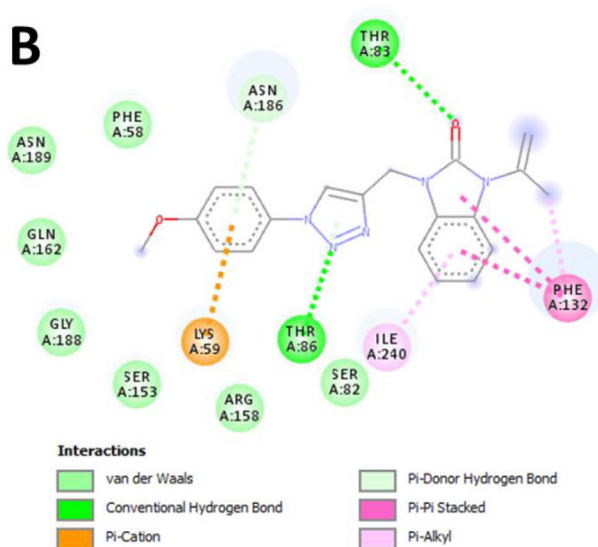
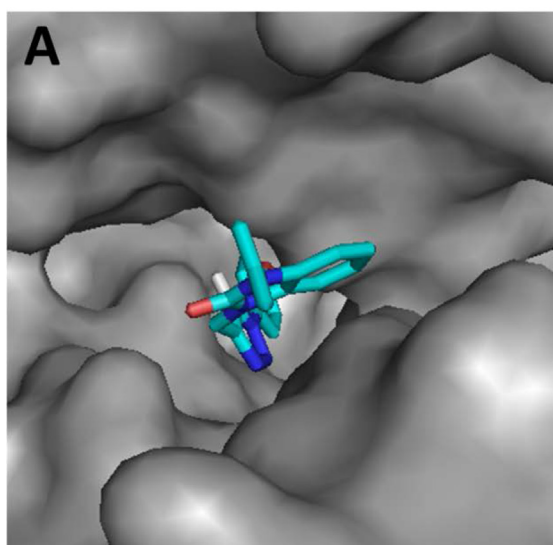


Fig. 3 A) Top view of the accessible surface of Threonine synthase from *B. subtilis* ATCC 6633 (PDB: 6CGQ) active site. B) Schematic representation of different interactions of **5b** within the catalytic cavity.

point of view, based on studies of molecular docking, the complex Threonine synthase-Ligand becomes stable by the formation of interactions between the amino acids forming the active site and the tested molecule, this is the case of our study by noticing the interactions formed and especially the intermolecular hydrogen bonds.

Concerning the complex: *E. coli*-ligand, docking studies predicted that compound **5b** would be the most active, with the lowest energy value (7.80 kcal/mol) when compared to other derivatives. **5b** through its triazole pharmacophore showed H-bonding interaction with the side chain of GLN88 and SER161. The 1-isopropenyl-2-benzimidazolidinone fragment in turn displayed a Pi-Sigma interaction with Val108, Alkyl and Pi-Alkyl with LEU106 and Pi-Donor hydrogen bond with TYR97. **5b** via its 4-methoxyphenyltriazole moiety exhibited a Pi-Alkyl interaction with VAL159 and Pi-Donor hydrogen bonds with amino acids: THR155 and SER161. Fig. 4. The results of the antibacterial assays are in accordance with the results from the molecular modeling calculations excellently. Thus, the 1,2,3-triazole linked benzimidazolidinone derivative is able to enter the enzyme pocket by showing significant binding interactions.

2.3.3. Antifungal activity

Using the diffusion method, all newly synthesized compounds were inspected for antifungal activity against two fungi (*A. fumigatus* and *A. brasiliensis*) and two yeast strains (*C. albicans* and *C. neoformans*) (Murray et al., 1995). Antifungal activity of compounds was compared with the nystatin reference and the results of this study were presented in Table 4. The inhibition zone of strains ranged from 9 mm to 27 mm for fungi and 11 mm to 20 mm for yeast. These results show that more compounds show stronger inhibition against fungal strains. More specifically, the compound **5b** with methoxy-groups at the *para* position of phenyl ring of benzimidazolone exhibit the strongest inhibition compared to other products against *A. brasiliensis* and *A. fumigatus* (between 27 mm and 26 mm), which make them even more efficient than the stan-

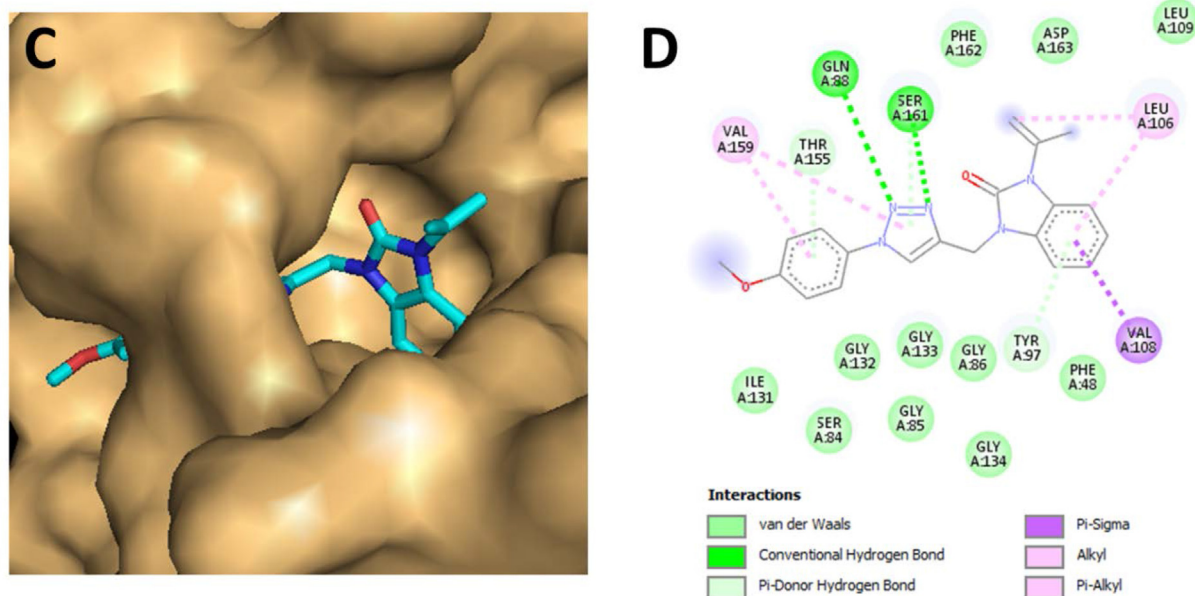


Fig. 4 C) Top view of the accessible surface of Escherichia coli (PDB: 3 T88) active site. D) Schematic representation of different interactions of **5b** within the catalytic cavity.

dard nystatin (Table 4). Moreover, the results of the biological activity showed also that compound **5a** bearing the *p*-chloro substituted benzene moiety significantly increase the activity followed by compound **5f** having 2-methoxyphenyl group while derivatives **5c**, **5d** and **5e** methyl-substituted did not show good inhibition value against all strains used. In summary, may account for the observed antifungal activity may be due to the chemical structure of the produced compounds having methoxy group or halogen such as chlorine atom in addition to the 1,2,3-triazole linked benzimidazolidinone core.

2.3.4. In vitro anti-Inflammatory activity

Protein denaturation is a well-known source of inflammation. When a protein is denatured, it loses its secondary and tertiary structures due to external stresses such heat, strong acids or bases, concentrations of inorganic salts, or organic solvents. The majority of biological proteins also lose their biological activity (Mizushima et al., 1968, Grant et al., 1970). In the current study, the inhibition of albumin denaturation method was used to assess the in vitro anti-inflammatory activity of all

derivatives **5a-f** and the reference drug Aspirin. As shown in Table 5, the results clearly indicate that some derivatives have significantly good inhibition. Besides to the tirazole tethered with benzimidazolidinone, the substituents introduced into the phenyl ring directly related to the triazole heterocycle have an effect on the activity. Indeed, compound **5a** with chlorine atom displayed better anti-inflammatory potential at different concentrations compared to its analogues and with values very close to those of Aspirin. This observation demonstrates the importance of halogens in the anti-inflammatory potency in particular the chlorine atom. On the other hand, the 4-methoxy derivative **5b** displayed good inhibitory values followed by 2-methoxy derivative **5f** while the compounds **5c**, **5d** and **5e** with methyl group showed moderate activity. We can conclude from the above findings that the mesomeric electron donor effect can enhance the anti-inflammation, this is the case of methoxy group and chlorine atom whereas the methyl group exerted just an inductive donor effect that's why did not show significant activity.

Table 4 Estimation of zone of inhibition of synthesized compounds against different fungal and yeasts strains.

Standard and Test compound	Zone of inhibition in mm			
	<i>A. brasiliensis</i>	<i>A. fumigatus</i>	<i>C. albicans</i>	<i>C. neoformans</i>
5a:4Cl	26	24	17	19
5b: 4OCH ₃	27	26	20	17
5c: 2,6-diCH ₃	11	11	14	13
5d:4CH ₃	10	9	12	13
5e: 2CH ₃	10	10	12	11
5f:2OCH ₃	19	20	16	15
Nystatin	25	24	22	23

Table 5 In vitro anti-inflammatory activity of benzimidazolidinone derivatives and aspirin by inhibition of albumin denaturation method.

Standard and Test compound	Concentration µg/mL				
	200	400	600	800	1000
5a:4-Cl	57.22	64.75	65.12	67.75	73.89
5b: 4-OCH ₃	52.37	61.33	62.32	65.69	70.17
5c: 2,6-diCH ₃	09.04	12.47	18.27	22.28	24.34
5d:4-CH ₃	10.23	12.64	15.19	18.22	20.41
5e: 2-CH ₃	09.15	10.24	13.73	16.38	19.56
5f:2-OCH ₃	44.12	49.24	51.85	52.14	59.69
Aspirin	59.36	66.13	67.62	69.48	75.23

Table 6 Docking binding energies (kcal/mol) of promising anti-inflammatory agents.

Compound	Free binding energy of pdb: 3IAZ (kcal mol ⁻¹)
5a	-7.9
5b	-7.5
5c	-7.6
5d	-7.4
5e	-7.5
5f	-7.7
Aspirin	-6.3

2.3.5. Molecular docking for anti-inflammatory activity

Our attention was next directed to assess the selectivity of our developed compounds 5a-f based on molecular docking by comprehending their docking with the inflammatory target receptor (PDB: 3IAZ). Table 6 demonstrates that derivative

5a has the lowest energy value (-7.90 kcal/mol) in comparison with its analogues even compared to the reference ligand Aspirin. According to Fig. 5, it was observed that the most active compound **5a** bounded to the active *via* several interesting interactions. The triazole ring was in interaction with THR430, PRO593 and TYR660 conventional Hydrogen bond, Pi-Donor hydrogen bond, Pi-Alkyl and Pi-Pi T-shaped interactions respectively. Moreover, **5a** through its benzimidazolidinone pharmacophore is involved in Alkyl and Pi-Alkyl interactions with VAL591. In addition, the 4-chlorophenyl moiety interacted with PRO655 by an Alkyl interaction. Inspired by the previous observations, molecular modeling agrees well with *in vitro* results of anti-inflammatory activity.

2.3.6. ADMET and predicted physicochemical properties

ADMET properties are known as key steps and appropriate methodologies used in drug development and discovery processes (Horchani et al., 2022b, Ye et al., 2019). Furthermore,

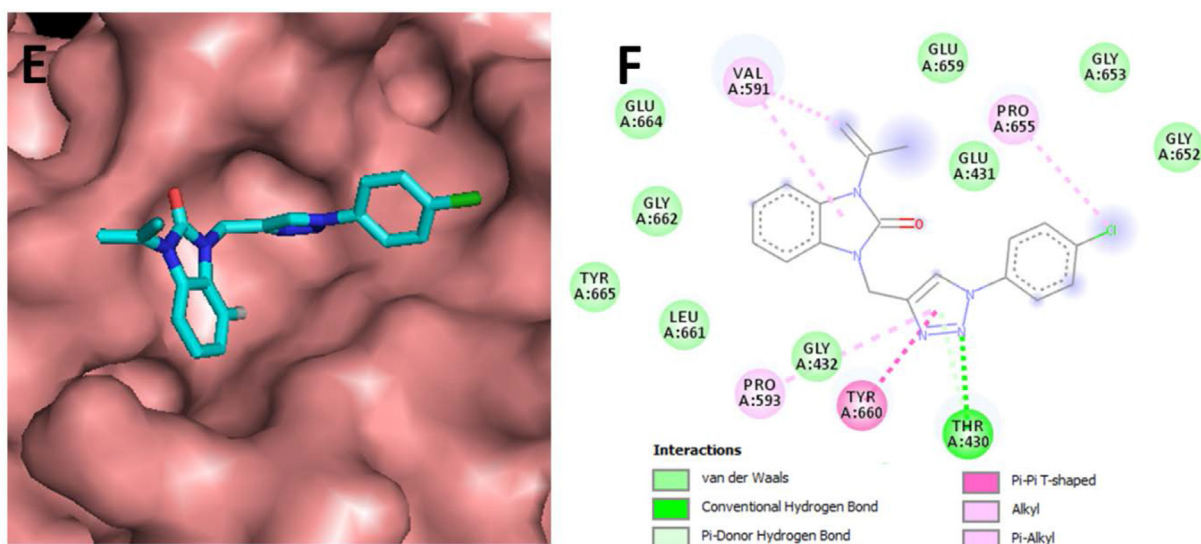


Fig. 5 E) Top view of the accessible surface of inflammatory protein (PDB: 3IAZ) active site. F) Schematic representation of different interactions of **5a** within the catalytic cavity.

Table 7 Predicted physicochemical properties for target compounds **5a-f**.

Compd. No.	MW ^a	nHA ^b	nHD ^c	logP(o/w) ^d	nrotbo ^e	TPSA ^f	MV ^g	%Abs ^h
Acceptable Value	< 500	< 10	< 5	< 5	= < 10	< 140	500	100 %
5a	365.100	6	0	4.350	4	57.640	355.575	89.11
5b	361.150	7	0	3.274	5	66.870	366.450	85.92
5c	358.190	6	1	3.497	4	64.420	377.162	86.77
5d	345.160	6	0	3.969	4	57.640	357.660	89.11
5e	345.160	6	0	3.984	4	57.640	357.660	89.11
5f	361.150	7	0	3.288	5	66.870	366.450	85.92

^a Molecular weight,

^b Number of hydrogen-bond acceptors,

^c Number of hydrogen-bond donors,

^d Octanol/water partition coefficient,

^e Number of rotatable bonds,

^f Topological polar surface area,

^g Molecular volume,

^h Percentage of absorption (%Abs = 109 - [0.345 × TPSA]).

the physicochemical properties are important parameters of a compound that influence efficacy, safety, or metabolism and can be predicted using Lipinski's rule of five (RO5), as summarized in Table 7. The rule of five (RO5) deals with the reliance of active compounds and defines the eight pharmacokinetics parameters named as the molecular weight, H-bond donors, H-bond acceptors, log P, number of rotatable bonds, topological polar surface area, molecular volume, percentage of absorption. So, these pharmacokinetic parameters are associated with the acceptable aqueous solubility. For more details, the predicted values of many properties categorized as molecular weight describe the size of the compound. In addition, the value of log P corresponds to the lipophilicity of the molecules which is matched to the solubility of the drug molecule in the aqueous medium. Accordingly, the higher the solubility, the higher the activity of the therapeutic agents. Moreover, the parameters of the H-bond donor and H-bond acceptor signalize the quantification of all atoms (N, O) besides to their efficiency in the formation of the hydrogen bond. Thus, the results obtained from the ADMET analysis with ADMETlab 2.0 software unveiled that the predicted compounds **5a-f** fully obeyed Lipinski's rule of five. These findings suggest that these synthesized analogues are feasible in order to serve as a future biological candidates.

3. Conclusion

In summary, we have designed a step-by-step synthetic route to build a novel series of 1,2,3-triazole linked benzimidazolidinone **5a-f** which was synthesized in good yields, by click reaction. New hybrid compounds were efficiently characterized by ^1H NMR, ^{13}C NMR, HRMS, and the structure of precursor **5b** was supported by X-ray crystallographic data. The synthesized compounds **5a-f** were evaluated biologically against antimicrobial and anti-inflammatory activities. The biological studies reveal that synthesized compounds may be classified as antimicrobial agents. Biological activity tests showed also that the synthesized compounds have moderate to good activity against anti-inflammatory. In addition, molecular docking simulations confirmed that the most active compounds have been well fitted in the active site of target enzymes *via* desirable interactions.

4. Experimental section

4.1. Chemistry

4.1.1. General information

The purity of products was confirmed by TLC using aluminium sheets (silica gel 60 F254) purchased from Merck. ^1H and ^{13}C NMR spectra were recorded on Bruker AC-400 in deuteriochloroform or DMSO d_6 solution. Chemical shifts are taken in ppm using TMS as an internal standard. High resolution mass spectra (HRMS) were recorded using Micromass LCT mass spectrometers (ESI technique, positive mode). Melting temperatures were determined in open glass capillaries and are not corrected. All chemical shifts values were reported in ppm and coupling constants are taken in Hz. Different signals multiplicities are described as following: s (singlet), d (doublet), t (triplet), m (multiplet) etc. All reaction mixture were monitored by TLC and purified by column chromatography using silica gell (40–63 μm).

Reagent and commercial products were purchased from Sigma Aldrich without prior purification. The starting material (**2**) was formed according to the literature. (Li et al., 2010).

4.1.2. General procedure A for the synthesis of 1-(prop-1-en-2-yl)-3-(prop-2-yn-1-yl)-1H-benzodimidazol-2(3H)-one **3**

To a solution of 1-(prop-1-en-2-yl)-1H-benzodimidazol-2(3H)-one (**2**) (4 g, 0.023 mol) in acetonitrile (70 mL) was added potassium carbonate (3.87 g, 0.028 mol). The reaction mixture was refluxed at 70 °C for 30 min before addition 1.2 equiv. of propargyl bromide (3.33 g, 0.028 mol). Then, the residue was extracted with ethyl acetate (120 mL \times 3). The organic extracts were dried and filtered. The crude was evaporated under vacuum and recrystallized from cyclohexane to give **3** (4.75 g, 80 %).

4.1.2.1. 1-(prop-1-en-2-yl)-3-(prop-2-yn-1-yl)-1H-benzodimidazol-2(3H)-one (**3**). Prepared, according to general procedure A, Yield: 80 %, off-white solid; mp 141–143 °C. R_f = 0.30 [EtOAc/cyclohexane 3:7]. ^1H NMR (CDCl_3 , 400 MHz): δ 2.22 (s, 3H, J = 0.8 Hz, CH_3), 2.31 (t, 1H, J = 3.2 Hz, CH), 4.69 (d, 2H, J = 3.6 Hz, CH_2), 5.20 (d, 1H, J = 0.8 Hz, =CH), 5.35 (d, 1H, J = 0.8 Hz, =CH), 7.20–7.11 (m, 4H, H_{arom}). ^{13}C NMR (CDCl_3 , 75 MHz): δ 20.1, 72.7, 30.1, 76.6, 108.5, 109.1, 113.3, 121.7, 121.8, 128.6, 128.9, 137.9, 151.9. HRMS, (ESI) calcd $\text{C}_{13}\text{H}_{12}\text{N}_2\text{NaO}$ [$\text{M} + \text{Na}$] $^+$: 235.0802, found 235.0804.

4.1.3. General procedure B for the synthesis of 1,2,3-triazole derivatives (**5a-f**)

To a mixture of alkyne **3** (400 mg, 1.88 mmol) in DCM (50 mL) and an equimolar amount of aryl azides was added NET_3 (0.38 mL, 2.82 mmol) and CuI (0.5 mol%). The reaction mixture was stirred at rt for 24 h. The solution was extracted with dichloromethane (60 mL \times 3) and dried using Na_2SO_4 . After evaporation of the solvent under vacuum The crude was evaporated under vacuum and recrystallized from cyclohexane to give **5a-f**.

4.1.3.1. 1-((1-(4-chlorophenyl)-1H-1,2,3-triazol-4-yl)methyl)-3-(prop-1-en-2-yl)-1H-benzodimidazol-2(3H)-one (**5a**). Prepared, according to general procedure B, Yield; 74 %, white solid; mp 118–120 °C. R_f = 0.27 [EtOAc/cyclohexane 3:7]. ^1H NMR (CDCl_3 , 400 MHz): δ 2.23 (s, 3H, CH_3), 5.20 (d, 1H, =CH), 5.25 (s, 2H, CH_2), 5.36 (d, 1H, J = 1.2 Hz, =CH), 7.11 (m, 3H, H_{arom}), 7.33 (m, 1H, H_{arom}), 7.45 (d, 2H, J = 9 Hz, H_{arom}), 7.82 (d, 2H, J = 8.7 Hz, H_{arom}), 8.05 (s, 1H, $\text{H}_{\text{triazole}}$). ^{13}C NMR (CDCl_3 , 75 MHz): δ 20.2, 36.3, 76.58, 77.42, 93.7, 108.7, 109.1, 113.2, 120.9, 121.7, 122.0, 128.8, 128.9, 136.5, 137.8, 138.8, 152.5. HRMS, (ESI) calcd $\text{C}_{19}\text{H}_{16}\text{ClN}_5\text{NaO}$ [$\text{M} + \text{Na}$] $^+$: 388.0134, found 388.0128.

4.1.3.2. 1-((1-(4-methoxyphenyl)-1H-1,2,3-triazol-4-yl)methyl)-3-(prop-1-en-2-yl)-1H-benzodimidazol-2(3H)-one (**5b**). Prepared, according to general procedure B, Yield; 68 %, off-white solid; mp 130–132 °C. R_f = 0.27 [EtOAc/cyclohexane 3:7]. ^1H NMR (CDCl_3 , 400 MHz): δ 2.24 (s, 3H, CH_3), 3.84 (s, 3H, OCH_3), 5.20 (s, 1H, =CH), 5.25 (s, 2H, CH_2), 5.35 (s, 1H, =CH), 7.97 (d, 2H, J = 9 Hz, H_{arom}).

7.10 (m, 3H, H_{arom}), 7.35 (m, 1H, H_{arom}), 7.57 (d, 2H, $J = 9$ Hz, H_{arom}), 7.97 (s, 1H, H_{triazole}). ¹³C NMR (CDCl₃, 75 MHz): δ 20.2, 36.3, 55.6, 108.7, 109.1, 113.2, 121.7, 122.0, 128.8, 128.9, 129.6, 130.7, 133.4, 137.8, 138.8, 152.5. HRMS, (ESI) calcd C₂₀H₁₉N₅NaO₂ [M + Na]⁺: 384.1224, found 384.1220.

4.1.4. 1-((1-(2,6-dimethylphenyl)-1H-1,2,3-triazol-4-yl)methyl)-3-(prop-1-en-2-yl)-1H-benzodimidazol-2(3H)-one (5c)

Prepared, according to general procedure **B**, Yield; 69 %, off-white solid; mp 122–124 °C. R_f = 0.28 [EtOAc/cyclohexane 3:7]. ¹H NMR (CDCl₃, 400 MHz): δ 1.94 (s, 6H, 2CH₃), 2.23 (s, 3H, CH₃), 5.21 (s, 1H, =CH), 5.31 (s, 2H, CH₂), 5.35 (d, 1H, $J = 1.2$ Hz, =CH), 7.10 (m, 3H, H_{arom}), 7.13 (d, 2H, $J = 8.4$ Hz, H_{arom}), 7.24 (m, 2H, H_{arom}), 7.29 (m, 2H, H_{arom}), 7.63 (s, 1H, H_{triazole}). ¹³C NMR (CDCl₃, 75 MHz): δ 17.4, 20.2, 36.7, 108.7, 109.1, 113.1, 121.6, 121.8, 128.4, 128.9, 129.1, 130.1, 135.3, 135.7, 137.9, 152.6. HRMS, (ESI) calcd C₂₁H₂₁N₅NaO [M + Na]⁺: 382.1637, found 382.1638.

4.1.4.1. 1-(prop-1-en-2-yl)-3-((1-(p-tolyl)-1H-1,2,3-triazol-4-yl)methyl)-1H-benzodimidazol-2(3H)-one (5d). Prepared, according to general procedure **B**, Yield; 70 %, white solid; mp 137–139 °C. R_f = 0.28 [EtOAc/cyclohexane 3:7]. ¹H NMR (CDCl₃, 400 MHz): δ 2.24 (s, 3H, CH₃), 2.39 (s, 3H, CH₃), 5.23 (m, 3H, =CH and CH₂), 5.36 (s, 1H, =CH), 7.09 (m, 3H, H_{arom}), 7.27 (d, 2H, $J = 8.7$ Hz, H_{arom}), 7.35 (d, 1H, $J = 5.7$ Hz, H_{arom}), 7.56 (d, 2H, $J = 8.4$ Hz, H_{arom}), 8.14 (s, 1H, H_{triazole}). ¹³C NMR (CDCl₃, 75 MHz): δ 20.2, 21.0, 36.3, 108.8, 109.1, 113.1, 120.4, 121.6, 121.9, 128.8, 129.0, 130.2, 137.9, 138.9, 152.6. HRMS, (ESI) calcd C₂₀H₁₉N₅NaO₄ [M + Na]⁺: 368.0482, found 368.0482.

4.1.4.2. 1-(prop-1-en-2-yl)-3-((1-(o-tolyl)-1H-1,2,3-triazol-4-yl)methyl)-1H-benzodimidazol-2(3H)-one (5e). Prepared, according to general procedure **B**, Yield; 72 %, off-white solid; mp 108–110 °C. R_f = 0.26 [EtOAc/cyclohexane 3:7]. ¹H NMR (CDCl₃, 400 MHz): δ 2.19 (s, 3H, CH₃), 2.23 (s, 3H, CH₃), 5.21 (s, 1H, =CH), 5.29 (s, 2H, CH₂), 5.35 (d, 1H, $J = 1.2$ Hz, =CH), 7.12 (m, 3H, H_{arom}), 7.28 (d, 1H, $J = 1.2$ Hz, H_{arom}), 7.29 (m, 1H, H_{arom}), 7.33 (m, 1H, H_{arom}), 7.35 (m, 1H, H_{arom}), 7.39 (m, 1H, H_{arom}), 7.79 (s, 1H, H_{triazole}). ¹³C NMR (CDCl₃, 75 MHz): δ 17.9; 20.2; 36.4; 108.8; 109.1; 113.2; 121.7; 121.9; 125.9, 126.8, 128.9, 129.1, 129.9, 131.5, 133.7, 137.9, 152.6. HRMS, (ESI) calcd C₂₀H₁₉N₅NaO [M + Na]⁺: 368.1482, found 368.1482.

4.1.4.3. 1-((1-(2-methoxyphenyl)-1H-1,2,3-triazol-4-yl)methyl)-3-(prop-1-en-2-yl)-1H-benzodimidazol-2(3H)-one (5f). Prepared, according to general procedure **B**, Yield; 68 %, off-white solid; mp 113–115 °C. R_f = 0.24 [EtOAc/cyclohexane 3:7]. ¹H NMR (CDCl₃, 400 MHz): δ 2.22 (s, 3H, CH₃), 3.82 (s, 3H, OCH₃), 5.33 (m, 4H, H_{arom}), 7.06 (m, 5H, H_{arom}), 7.36 (m, 2H, H_{arom}), 7.72 (d, 1H, $J = 8.0$ Hz, H_{arom}), 8.22 (s, 1H, H_{triazole}). ¹³C NMR (CDCl₃, 75 MHz): δ 20.1, 36.3, 55.9, 109.2, 109.5, 112.2, 121.2, 121.7, 121.9, 122.3, 125.4, 127.6, 129.9, 130.2, 137.7, 151.1. HRMS, (ESI) calcd C₂₀H₁₉N₅NaO₂[M + Na]⁺: 384.1428, found 384.1424.

4.2. Biological activity

4.2.1. Antibacterial screening

By using the Agar Well Diffusion Assay technique, the antibacterial properties of the synthesized compounds were assessed against two Gram-positive bacteria, i.e., *S. aureus* and *B. subtilis*, and two Gram-negative bacteria, i.e., *S. typhi* and *E. coli*. These pathogenic strains were grown for 24 h at 37 °C on nutrient agar. In 10 mL of physiological medium, colonies were suspended, and mixed for 5 min, and the suspensions were calibrated to 0.5 McFarland standard turbidity. Muller Hinton Agar medium plates were covered with one millilitre of bacterial suspension and incubated for 30 min at 37 °C. The seeded agar plates were punched with wells that were approximately 6 mm in diameter, and each test substance was then put to the wells after being reconstituted in DMSO. For all of the test substances, DMSO served as the control. The plates were kept at room temperature for two hours to allow the chemicals to diffuse into the agar before the plates were incubated at 37 °C for 24 h. By using a digital calliper, the diameters of the clear zones of inhibition surrounding the sample were measured after 24 h.

4.2.2. Antifungal activity

Yeasts Strains: two yeast strains, *C. albicans* and *C. neoformans*, were cultivated on Sabouraud agar for 48 h at 37 °C (the ideal temperature for bacterial growth). The suspensions of pure colonies were then adjusted to 0.5 McFarland standard turbidity after being suspended in 10 mL of physiological medium and well stirred for 5 min. Plates of Sabouraud agar medium received one milliliter of yeast suspension, which was then incubated at 37 °C for 30 min. Then, using a sterile glassy borer, 6 mm diameter wells were drilled into the agar medium. The synthesized compounds were produced in DMSO (1 mg/mL) and added to the appropriate wells; as a control, DMSO was added to one of the wells. For 48 h, these plates were kept in an incubator at 37 °C to promote yeast growth. By using a digital calliper, the diameters of the clear zones of inhibition surrounding the sample were measured after 48 h.

Fungal Strains: two fungi strains, *A. brasiliensis* and *A. fumigatus* were cultured on inclined Sabouraud agar in Falcon tube 15 mL at 25 °C for 7 days (optimal temperature for their growing). The fungus strain's spore was measured at 10⁶ spores/mL after being suspended in peptone water. After that, Sabouraud agar medium plates were covered with one millilitre of the fungal suspension and incubated at 25 °C for 30 min. Then, using a sterile glassy borer, 6 mm diameter wells were drilled in agar media. The synthesized compounds were produced in DMSO (1 mg/mL) and added to the appropriate wells; as a control, DMSO was added to one of the wells. For five days, these plates were kept in an incubator at 25 °C to promote fungi development. After five days, a digital caliper was used to measure the diameters of the clear zone of inhibition surrounding the sample.

4.2.3. In vitro anti-inflammatory activity

The anti-inflammatory activity of benzimidazolone derivatives **5a–f** was determined as below:

Various concentrations of 2 mL of each compound was mixed individually with 3 mL of sodium phosphate buffer saline (pH 6.4) containing 0.2 mL of eggs albumin yielding a final

volume of 5 mL. The pure blank does not contain the substrate, but will be added 3 mL of buffer solution. All compounds were re-suspended in the DMSO followed by dilution in the buffer in order that the DMSO does not exceed 1 %. Control was given a comparable volume of double-distilled water. The mixture was then heated at 70 °C for 5 min after being incubated at 37 °C for about 15 min and the absorbance was determined at 660 nm after cooling. To determine absorbance, aspirin (a standard medication) was used as positive control and as a reference medication and handled accordingly. Using the formula listed below, the % inhibition of protein denaturation was determined:

Percentage inhibition

$$= (\text{Abs Control} - \text{abs Sample}) \times 100 / \text{Abs control}$$

4.3. Molecular docking procedure

Molecular docking simulations were performed by Auto Dock 4.2 program package (Trott et al., 2010). The optimization of all the geometries of compounds was carried out using ACD (3D viewer) software (<https://www.filefacts.com/acd3d-viewer-freeware-info>). The three dimensional structure of PDB (PDB: 6CGQ) (Petronikolou et al., 2019) and (PDB: 3 T88) (Li et al., 2011) for the antibacterial activity and of PDB (PDB: 3IAZ) (Mir et al., 2009) for the anti-inflammatory potential were obtained from the RSCB protein data bank. First, the water molecules were eliminated and the missing hydrogens and Gasteiger charges were then added to the system during the preparation of the receptor input file. Next, AutoDock Tools were used for the preparation of the corresponding ligand and protein files (PDBQT). Then, pre-calculation of the grid maps was performed using Auto Grid for saving a lot of time during docking. The visualization and analysis of interactions were performed using Discovery Studio 2017R2 (<https://www.3dsbiovia.com/products/collaborative-science/biovia-discovery-studio/>).

4.4. ADMET properties

To predict the pharmacokinetic properties: molecular weight, number of hydrogen-bond acceptors, Number of hydrogen-bond donors, octanol/water partition coefficient, number of rotatable bonds, topological polar surface area, molecular volume and percentage of absorption of all synthesized derivatives, the chemoinformatic tools (database): ADMETlab 2.0 (<https://admetmesh.scbdd.com/service/evaluation/cal/>) was used.

Declaration of Competing Interest

The authors declare that they have no known competing financial interests or personal relationships that could have appeared to influence the work reported in this paper.

Acknowledgments

The authors extend their appreciation to Princess Nourah bint Abdulrahman University Researchers Supporting Project number (PNURSP2023R95), Princess Nourah bint Abdulrahman University, Riyadh, Saudi Arabia.

Fundings

This research was funded by Princess Nourah bint Abdulrahman University Researchers Supporting Project number (PNURSP2023R95), Princess Nourah bint Abdulrahman University, Riyadh, Saudi Arabia.

Appendix A. Supplementary material

Supplementary data to this article can be found online at <https://doi.org/10.1016/j.arabjc.2023.104566>.

References

- Ali, A.A., Konwar, M., Chetia, M., Sarma, D., 2016. [Bmim]OH mediated Cu-catalyzed azide-alkyne cycloaddition reaction: a potential green route to 1,4-disubstituted 1,2,3-triazoles. *Tetrahedron Lett.* 57, 5661–5665. <https://doi.org/10.1016/j.tetlet.2016.11.014>.
- Ankali, K.N., Rangaswamy, J., Shalavadi, M., Naik, N., Krishnamurthy, G.N., 2021. Synthesis and molecular docking of novel 1,3-Thiazole Derived 1,2,3-Triazoles and in vivo biological evaluation for their anti anxiety and anti inflammatory activity. *J. Mol. Struct.* 1236. <https://doi.org/10.1016/j.molstruc.2021.130357> 130357.
- Arif, K., Fatima, N., Rafia, B., Deepak, D., Piyush, B., Majeed, S., Bilal, A.L., Yuba, R.P., Qazi, N.A., Shazia, P., Intzar, A., Shashank, K.S., Gousia, C., Syed, S., 2022. 1,2,3-Triazole Tethered Hybrid Capsaicinoids as Antiproliferative Agents Active against Lung Cancer Cells (A549). *ACS Omega* 36, 32078–32100. <https://doi.org/10.1021/acsomega.2c03325>.
- Atena, S.R., Jamshid, M., Majid, D., Mohammad Reza, S., Jamshidkhan, C., 2021. Oil-in-water nanoemulsions comprising Berberine in olive oil: biological activities, binding mechanisms to human serum albumin or holo-transferrin and QMMD simulations. *J. Biomol. Struct. Dyn.* 39, 1029–1043. <https://doi.org/10.1080/07391102.2020.1724568>.
- Banerji, B., Pramanik, S.K., 2015. Synthesis and cytotoxicity studies of 1-propenyl-1,3-dihydro-benzimidazol-2-one. *J. Chem. Biol.* 8, 73–78. <https://doi.org/10.1007/s12154-015-0130-8>.
- Bozorov, K., Zhao, J., Aisa, H.A., 2019. 1,2,3-Triazole-containing hybrids as leads in medicinal chemistry: A recent overview. *Bioorg. Med. Chem.* 27, 3511–3531. <https://doi.org/10.1016/j.bmc.2019.07.005>.
- Çelik, F., Ustabaş, R., Süleymanoğlu, N., Direkel, S., Güler, H.I., Ünver, Y., 2021. 1,2,3-triazole derivative: Synthesis, characterization, DFT, molecular docking study and antibacterial-antileishmanial activities. *J. Indian Chem. Soc.* 98. <https://doi.org/10.1016/j.jics.2021.100105> 100105.
- Chamani, J., Moosavi-Movahedi, A.A., 2006. Effect of n-alkyl trimethylammonium bromides on folding and stability of alkaline and acid-denatured cytochrome c: a spectroscopic approach. *J. Colloid. Interface Sci.* 297, 561–569. <https://doi.org/10.1016/j.jcis.2005.11.035>.
- Darroudi, M., Hamzehloueian, M., Sarrafi, Y., 2021. An experimental and mechanism study on the regioselective click reaction toward the synthesis of thiazolidinone-triazole. *Heliyon*. 7, e06113.
- Dolomanov, O.V., Bourhis, L.J., Gildea, R.J., Howard, J.A.K., Puschmann, H., 2009. Olex2: A complete structure solution, refinement and analysis program. *J. Appl. Cryst.* 42, 339–341. <https://doi.org/10.1107/S0021889808042726>.
- Duarte, W.R., da Silva, L.P., Buss, J.H., Goldani, B.S., Fronza, M., Segatto, N.V., Alves, D., Savegnagoc, L., Seixas, F.K., Collares, T., 2017. Apoptosis induction by 7-chloroquinoline-1,2,3-triazolyl carboxamides in triple negative breast cancer cells. *Biomed.*

- Pharmacother. 91, 510–516. <https://doi.org/10.1016/j.biopha.2017.04.098>.
- El-Naggar, M., Eldehna, W., Almahli, H., Elgez, A., Fares, M., Elaasser, M., Abdel-Aziz, H., 2018. Novel Thiazolidinone/Thiazolo [3,2-a] Benzimidazolone-Isatin conjugates as apoptotic anti-proliferative agents towards breast cancer: one-pot synthesis and in vitro biological evaluation. *Molecules*. 23, 1420. <https://doi.org/10.3390/molecules23061420>.
- Feng, L.-S., Zheng, M.-J., Zhao, F., Liu, D., 2021. 1,2,3-Triazole hybrids with anti-HIV-1 activity. *Arch. Pharm.* 354, 2000163. <https://doi.org/10.1002/ardp.202000163>.
- Fonseca, F.S., Carrão, D.B., de Albuquerque, N.P., Nardini, V., Dias, L.G., da Silva, R.M., Lopes, N.P., de Oliveira, A.R.M., 2020. Myclobutanil enantioselective risk assessment in humans through in vitro CYP450 reactions: Metabolism and inhibition studies. *Food Chem. Toxicol.* 128, 202–211. <https://doi.org/10.1016/j.fct.2019.04.009>.
- Grant, N.H., Album, H.E., Kryzanasukas, C., 1970. Stabilization of serum albumin by anti-inflammatory drugs. *Biochem. Pharmacol.* 19, 715–722. [https://doi.org/10.1016/0006-2952\(70\)90234-0](https://doi.org/10.1016/0006-2952(70)90234-0).
- Hamid, M., Fatemeh, H., Niloofar, S., Elahe, K., Bizhan, M.N., Parisa, M., Jamshidkhan, C., 2022. Glucokinase activity enhancement by cellulose nanocrystals isolated from jujube seed: A novel perspective for type II diabetes mellitus treatment (*In vitro*). *J. Mol. Struct.* 1269,. <https://doi.org/10.1016/j.molstruc.2022.133803>.
- Harish, C.U., 2021. Coumarin-1,2,3-triazole hybrid molecules: an emerging scaffold for combating drug resistance. *Curr. Top Med. Chem.* 21, 737–752. <https://doi.org/10.2174/1568026621666210303145759>.
- Horchani, M., Hajlaoui, A., Harrath, A.H., Mansour, L., Ben Jannet, L., Romdhane, A., 2020. New pyrazolo-triazolo-pyrimidine derivatives as antibacterial agents: design and synthesis, molecular docking and DFT studies. *J. Mol. Struct.* 1199,. <https://doi.org/10.1016/j.molstruc.2019.127007>.
- Horchani, M., Edziri, H., Harrath, A.H., Ben Jannet, H., Romdhane, A., 2022a. Access to new Schiff bases tethered with pyrazolopyrimidinone as antibacterial agents: design and synthesis, molecular docking and DFT analysis. *J. Mol. Struct.* 1248,. <https://doi.org/10.1016/j.molstruc.2021.131523>.
- Horchani, M., Heise, N.V., Csuk, R., Ben Jannet, H., Harrath, A.H., Romdhane, A., 2022b. Synthesis and In Silico Docking Study towards M-Pro of Novel Heterocyclic Compounds Derived from Pyrazolopyrimidinone as Putative SARS-CoV-2 Inhibitors. *Molecules* 27, 5303. <https://doi.org/10.3390/molecules27165303>.
- Ibrahim, S., Ghabi, A., Amiri, N., Mtiraoui, H., Hajji, M., Bel-Hadj-Tahar, R., Msaddek, M., 2021. Microwave-assisted synthesis of (3,5-disubstituted isoxazole)-linked benzimidazolone derivatives: DFT calculations and biological activities. *Monatshefte Für Chemie - Chemical Monthly*. 152, 523–535. <https://doi.org/10.1007/s00706-021-02764-0>.
- Intagliata, S., Sharma, A., King, T.I., Mesangeau, C., Seminerio, M., Chin, F.T., Wilson, L.L., Matsumoto, R.R., McLaughlin, J.P., Avery, B.A., McCurdy, C.R., 2020. Discovery of a Highly Selective Sigma-2 Receptor Ligand, 1-(4-(6,7-Dimethoxy-3,4-dihydroisoxolin-2(1H)-yl)butyl)-3-methyl-1H-benzod[imidazol-2(3H)-one (CM398), with Drug-Like Properties and Antinociceptive Effects In Vivo. *AAPS J.* 22. <https://doi.org/10.1208/s12248-020-00472-x>.
- Jagannath, K.V., Krishnamurthy, G., 2021. Design, Synthesis, and Anti-Tubercular Studies of 10-(phenylsulfonyl)pyrimido[1,2-a]benzimidazol (10H) One Derivatives. *New Innovations Chem. Biochem.* 3, 66–75. <https://doi.org/10.9734/bpi/nicb/v3/13631D>.
- Kamalraj, V.R., Senthil, S., Kannan, P., 2008. One-pot synthesis and the fluorescent behavior of 4-acetyl-5-methyl-1,2,3-triazole regioisomers. *J. Mol. Struct.* 892, 210–215. <https://doi.org/10.1016/j.molstruc.2008.05.028>.
- Khalili, J.S., Zhu, H., Mak, N.S.A., Yan, Y., Zhu, Y., 2020. Novel coronavirus treatment with ribavirin: Groundwork for an evaluation concerning COVID-19. *J. Med. Virol.* 92, 740–746. <https://doi.org/10.1002/jmv.25798>.
- Li, S.K., Ji, Z.Q., Zhang, J.W., Guo, Z.Y., Wu, W.J., 2010. Synthesis of 1-Acyl-3-isopropenylbenzimidazolone Derivatives and Their Activity against *Botrytis cinerea*. *J. Agric. Food. Chem.* 58, 2668–2672. <https://doi.org/10.1021/jf903855y>.
- Li, H.J., Li, X., Liu, N., Zhang, H., Truglio, J.J., Mishra, S., Kisker, C., Garcia-Diaz, M., Tonge, P.J., 2011. Mechanism of the Intramolecular Claisen Condensation Reaction Catalyzed by MenB, a Crotonase Superfamily Member. *Biochemistry*. 50, 9532–9544. <https://doi.org/10.1021/bi200877x>.
- Lu, H., Shrivastava, M., Whiteway, M., Jiang, Y., 2021. *Candida albicans* targets that potentially synergize with fluconazole. *Crit. Rev. Microbiol.* 47, 323–337. <https://doi.org/10.1080/1040841X.2021.1884641>.
- Maryam, D., Zeinab, A.T., Narges, M., Reza, T., Sogand, A.F., Atiye, T., Negar, N.E., Mohammad, R.S., Jamshidkhan, C., 2020. A novel view of the separate and simultaneous binding effects of docetaxel and anastrozole with calf thymus DNA: Experimental and in silico approaches. *Spectrochim. Acta A Mol. Biomol. Spectrosc.* 228,. <https://doi.org/10.1016/j.saa.2019.117528>.
- Mavrova, T., Anichina, K.K., Vuchev, D.I., Tsenov, J.A., Kondeva, M.S., Micheva, M.K., 2005. Synthesis and antitrichinellosis activity of some 2-substituted-[1,3]thiazolo[3,2-a]benzimidazol-3(2H)-ones. *Bioorg. Med. Chem.* 13, 5550–5559. <https://doi.org/10.1016/j.bmc.2005.06.046>.
- Mir, R., Singh, N., Vikram, G., Kumar, R.P., Sinha, M., Bhushan, A., Kaur, P., Srinivasan, A., Sharma, S., Singh, T.P., 2009. The structural basis for the prevention of nonsteroidal antiinflammatory drug-induced gastrointestinal tract damage by the C-lobe of bovine colostrum lactoferrin. *Biophys. J.* 97, 3178–3186. <https://doi.org/10.1016/j.bpj.2009.09.030>.
- Miyata, A., Iwamoto, K., Kawano, N., Kohmura, K., Yamamoto, M., Aleksic, B., Ebe, K., Noda, A., Noda, Y., Iritani, S., Ozaki, N., 2014. The effects of acute treatment with ramelteon, triazolam, and placebo on driving performance, cognitive function, and equilibrium function in healthy volunteers. *Psychopharmacology*. 232, 2127–2137. <https://doi.org/10.1007/s00213-014-3843-4>.
- Mizushima, Y., Kobayashi, M., 1968. Interaction of anti-inflammatory drugs with serum proteins, especially with some biologically active proteins. *J. Pharm. Pharmacol.* 20, 169–173. <https://doi.org/10.1111/j.2042-7158.1968.tb09718.x>.
- Mujahid, M., Sadam, H., Bin, B.G., Kiramat, A.S., Faraz Khan, M., Muhammad, Y., Sadam, H., Farooq, A., 2021. Fabrication and characterization of rizatriptan loaded pullulan nanofibers as oral fast-dissolving drug system. *Mater. Res. Express*. 8,. <https://doi.org/10.1088/2053-1591/abff0b> 055404.
- Murray, P. R., Baron, E. J., Pfaller, M. A., Tenover, F. C. and Tenover, R. H., 1995. *Manual Clinical Microbiol*, sixth ed., ASM Press, Washington DC, pp. 1327-1341.
- Najmeh, Z.F., Zeinab, A.T., Atena, S.R., Parisa, M., Niknaz, N., Fatemeh, H., Hamid, R.R., Mohammad, R.S., Jamshidkhan, C., 2021. Determining the Interaction Behavior of Calf Thymus DNA with Anastrozole in the Presence of Histone H1: spectroscopies and Cell Viability of MCF-7 Cell Line Investigations. *DNA Cell Biol.* 40, 1039–1051. <https://doi.org/10.1089/dna.2021.0052>.
- Narges, M., Maryam, D., Maryam, A.L., Mahtab, P., Parisa, M., Zeinab, A.T., Mohammad, R.S., Jamshidkhan, C., 2022. Evaluation of the binding effect and cytotoxicity assay of 2-Ethyl-5-(4-methylphenyl) pyramido pyrazole ophthalazine trione on calf thymus DNA: spectroscopic, calorimetric, and molecular dynamics approaches. *Luminescence* 37, 310–322. <https://doi.org/10.1002/bio.4173>.

- Nemallapudi, B.R., Guda, D.R., Ummadi, N., Avula, B., Zyryanov, G.V., Reddy, C.S., Gundala, S., 2021. New Methods for Synthesis of 1,2,3-Triazoles: a review. *Polycycl. Aromat. Compd.* 1–19. <https://doi.org/10.1080/10406638.2020.1866038>.
- Nielsen, S., McAuley, A., 2020. Etizolam: A rapid review on pharmacology, non-medical use and harms. *Drug Alcohol Rev.* 39, 330–336. <https://doi.org/10.1111/dar.13052>.
- Nisha Poonia, N., Lal, K., Kumar, A., Kumar, A., Sahu, S., Baidya, A.T.K., Kumar, R., 2022. Urea-thiazole/benzothiazole hybrids with a triazole linker: synthesis, antimicrobial potential, pharmacokinetic profile and in silico mechanistic studies. *Mol. Divers.* 26, 2375–2391. <https://doi.org/10.1007/s11030-021-10336-x>.
- Nooshin, A., Vahid, S., Mohammad Reza, S., Jamshidkhan, C., 2016. Investigation of the interaction between human serum albumin and two drugs as binary and ternary systems. *Eur. J. Drug Metab. Pharmacokinet.* 41, 705–721. <https://doi.org/10.1007/s13318-015-0297-y>.
- Panebianco, M., Prabhakar, H., Marson, A.G., 2020. Rufinamide add-on therapy for drug-resistant epilepsy. *Cochrane Database Syst. Rev.* <https://doi.org/10.1002/14651858.CD011772.pub3>.
- Paredes-Zúñiga, S., Trost, N., De la Paz, J.F., Alcayaga, J., Allende, M.L., 2019. Behavioral effects of triadimefon in zebrafish are associated with alterations of the dopaminergic and serotonergic pathways. *Prog. Neuro-Psychopharmacol. Biol. Psychiatry.* 92, 118–126. <https://doi.org/10.1016/j.pnpbp.2018.12.012>.
- Petronikolou, N., Ortega, M.A., Borisova, S.A., Nair, S.K., Metcalf, W.W., 2019. Molecular Basis of *Bacillus subtilis* ATCC 6633 Self-Resistance to the Phosphono-oligopeptide Antibiotic Rhizocticin. *ACS Chem. Biol.* 14, 742–750. <https://doi.org/10.1021/acscchembio.9b00030>.
- Pribut, N., Basson, A.E., van Otterlo, W.A.L., Liotta, D.C., Pelly, S.C., 2019. Aryl Substituted Benzimidazolones as Potent HIV-1 Non-Nucleoside Reverse Transcriptase Inhibitors. *ACS Med. Chem. Lett.* 10, 196–202. <https://doi.org/10.1021/acsmchemlett.8b00549>.
- Rania, A., Singha, A., Kaur, J., Singh, G., Bhatti, R., Gumedde, N., Kisten, P., Singh, P., Sumanjit, K., 2021. 1H–1,2,3-triazole grafted tacrine-chalcone conjugates as potential cholinesterase inhibitors with the evaluation of their behavioral tests and oxidative stress in mice brain cells. *Bioorg. Chem.* 114, <https://doi.org/10.1016/j.bioorg.2021.105053> 105053.
- Reza, T., Nazanin, H., Yasaman, R., Sara, N., Farzaneh, S., Zeinab, A.T., Mohammad, R.S., Jamshidkhan, C., 2022. Exploring the HSA/DNA/lung cancer cells binding behavior of *p*-Synephrine, a naturally occurring phenyl ethanol amine with anti-adipogenic activity: multi spectroscopic, molecular dynamic and cellular approaches. *J. Mol. Liq.* 368, <https://doi.org/10.1016/j.molliq.2022.120826> 120826.
- Rolf, H., Günter, S., Leander, M., 1967. 1.3-Dipolare Cycloadditionen, XXXII. Kinetik der Additionen organischer Azide an CC-Mehrfachbindungen. *Chem. Ber.* 100, 2494–2507. <https://doi.org/10.1002/cber.19671000806>.
- Saber, A., Anouar, E.H., Sebbar, G., Ibrahim, B.E., Srhir, M., Hökelek, T., Maguef, J.T., El Ghayati, L., Sebbar, N.K., Essassi, E.M., 2021b. New 1,2,3-triazole containing benzimidazolone derivatives: Syntheses, crystal structures, spectroscopic characterizations, Hirshfeld surface analyses, DFT calculations, anti-corrosion property anticipation, and antibacterial activities. *J. Mol. Struct.* 1242, <https://doi.org/10.1016/j.molstruc.2021.130719> 130719.
- Saber, A., Anouar, E.H., Sebbar, G., El Ibrahim, B., Srhir, M., Hökelek, T., Maguef, J.T., El Ghayati, L., Sebbar, N.K., Essassi, E.M., 2021a. New 1,2,3-triazole containing benzimidazolone derivatives: Syntheses, crystal structures, spectroscopic characterizations, Hirshfeld surface analyses, DFT calculations, anti-corrosion property anticipation, and antibacterial activities. *J. Mol. Struct.* <https://doi.org/10.1016/j.molstruc.2021.130719>.
- Sarooha, B., Kumar, G., Kumar, R., Kumari, M., Kumar, S., 2022. a minireview of 1,2,3-triazole hybrids with O-heterocycles as leads in medicinal chemistry. *Chem. Biol. Drug Des.* 100, 843–869. <https://doi.org/10.1111/cbdd.13966>.
- Sattar, K.M., Sara, E.T., Melika, K.V., Parisa, J., Parisa, M., Helya, Y., Zeinab, A.T., Mohammad, R.S., Jamshidkhan, C., 2022. Novel perspective into the interaction behavior study of the cyanidin with human serum albumin-holo transferrin complex: Spectroscopic, calorimetric and molecular modeling approaches. *J. Mol. Liq.* 356, <https://doi.org/10.1016/j.molliq.2022.119042> 119042.
- Sheldrick, G.M., 2015a. Crystal structure refinement with ShelXL. *Acta Cryst.* C71, 3–8. <https://doi.org/10.1107/S2053229614024218>.
- Sheldrick, G.M., 2015b. ShelXT-Integrated space-group and crystal-structure determination. *Acta Cryst.* A71, 3–8. <https://doi.org/10.1107/S2053273114026370>.
- Shi, J., Ju, R., Gao, H., Huang, Y., Guo, L., Zhang, D., 2022. Targeting glutamine utilization to block metabolic adaptation of tumor cells under the stress of carboxyamidotriazole-induced nutrients unavailability. *Acta Pharm. Sin. B.* 12, 759–773. <https://doi.org/10.1016/j.apsb.2021.07.008>.
- Silva, T.B., Ji, K.N., Pauli, F.P., Galvão, R.M., Faria, A.F., Bello, M. L., Resende, J.A., Campos, V.R., Forezi, L.daS.M., da Silva, F.D. C., Faria, R.X., 2021. Synthesis and in vitro and in silico studies of 1H- and 2H-1,2,3-triazoles as antichagasic agents. *Bioorg. Chem.* 116. <https://doi.org/10.1016/j.bioorg.2021.105250>.
- Tamma, P.D., Beisken, S., Bergman, Y., Posch, A.E., Avdic, E., Sharara, S.L., Cosgrove, E.S., Simmer, P.J., 2021. Modifiable Risk Factors for the Emergence of Ceftolozane-Tazobactam Resistance. *Clin. Infect. Dis.* 73, e4599–e4606. <https://doi.org/10.1093/cid/ciaa1306>.
- Trott, O., Olson, A.J., 2010. AutoDock Vina: improving the speed and accuracy of docking with a new scoring function, efficient optimization, and multithreading. *J. Comput. Chem.* 31, 455–461. <https://doi.org/10.1002/jcc.21334>.
- Valadas, J., Mocelin, R., Sacht, A., Marcon, M., Zanette, R.A., Dallegrave, E., Herrmann, A.P., Piato, A., 2019. Propiconazole induces abnormal behavior and oxidative stress in zebrafish. *Environ. Sci. Pollut. Res.* <https://doi.org/10.1007/s11356-019-05977-3>.
- Worthington, P.A., 1991. Synthesis of 1,2,4-triazole compounds related to the fungicides flutriafol and hexaconazole. *Pest. Sci.* 31, 457–498. <https://doi.org/10.1002/ps.2780310405>.
- Ye, Z., Yang, Y., Li, X., Cao, D., Ouyang, D., 2019. An Integrated Transfer Learning and Multitask Learning Approach for Pharmacokinetic Parameter Prediction. *Mol. Pharm.* 16, 533–541. <https://doi.org/10.1021/acs.molpharmaceut.8b00816>.
- Zahra, N., Mohammad, M., Mina, S., Elahe, K.-R., Najmeh, E., Mohammad, S., Mahnaz, K., Tahmineh, A., 2019. Novel tacrine-coumarin hybrids linked to 1,2,3-triazole as anti-Alzheimer's compounds: In vitro and in vivo biological evaluation and docking study. *Bioorg. Chem.* 83, 303–316. <https://doi.org/10.1016/j.bioorg.2018.10.056>.